JOURNAL OF VIROLOGY, Feb. 2006, p. 1077–1086 Vol. 80, No. 3
0022-538X/06/$08.00+0 doi:10.1128/JVI.80.3.1077–1086.2006

Identification of an NF-κB-Dependent Gene Network in Cells Infected by Mammalian Reovirus†

Sean M. O'Donnell,[1,2] Geoffrey H. Holm,[1,2] Janene M. Pierce,[3] Bing Tian,[4] Melissa J. Watson,[1,2]‡ Ravi S. Chari,[3] Dean W. Ballard,[5] Allan R. Brasier,[4,6] and Terence S. Dermody[1,2,5]*

Departments of Pediatrics,[1] Surgery,[3] and Microbiology and Immunology[5] and Elizabeth B. Lamb Center for Pediatric Research,[2] Vanderbilt University School of Medicine, Nashville, Tennessee 37232, and Department of Medicine[4] and Sealy Center for Molecular Sciences,[6] The University of Texas Medical Branch, Galveston, Texas 77555

Received 11 April 2005/Accepted 26 October 2005

Reovirus infection activates NF-κB, which leads to programmed cell death in cultured cells and in the murine central nervous system. However, little is known about how NF-κB elicits this cellular response. To identify host genes activated by NF-κB following reovirus infection, we used HeLa cells engineered to express a degradation-resistant mutant of IκBα (mIκBα) under the control of an inducible promoter. Induction of mIκBα inhibited the activation of NF-κB and blocked the expression of NF-κB-responsive genes. RNA extracted from infected and uninfected cells was used in high-density oligonucleotide microarrays to examine the expression of constitutively activated genes and reovirus-stimulated genes in the presence and absence of an intact NF-κB signaling axis. Comparison of the microarray profiles revealed that the expression of 176 genes was significantly altered in the presence of mIκBα. Of these genes, 64 were constitutive and not regulated by reovirus, and 112 were induced in response to reovirus infection. NF-κB-regulated genes could be grouped into four distinct gene clusters that were temporally regulated. Gene ontology analysis identified biological processes that were significantly overrepresented in the reovirus-induced genes under NF-κB control. These processes include the antiviral innate immune response, cell proliferation, response to DNA damage, and taxis. Comparison with previously identified NF-κB-dependent gene networks induced by other stimuli, including respiratory syncytial virus, Epstein-Barr virus, tumor necrosis factor alpha, and heart disease, revealed a number of common components, including CCL5/RANTES, CXCL1/GRO-α, TNFAIP3/A20, and interleukin-6. Together, these results suggest a genetic program for reovirus-induced apoptosis involving NF-κB-directed expression of cellular genes that activate death signaling pathways in infected cells.

Mammalian reoviruses have served as highly tractable models for studies of viral pathogenesis (59). Reoviruses are nonenveloped, icosahedral viruses with a genome consisting of 10 double-stranded RNA segments (37). Following attachment to cellular receptors (2, 7) and entry by receptor-mediated endocytosis (17, 50), reovirus replication occurs exclusively in the cytoplasm. Newborn mice infected with reovirus sustain injury to a variety of organs, including the central nervous system (CNS), heart, and liver (62). Reovirus induces the morphological and biochemical features of apoptosis in cultured cells (10, 60) and in vivo (11, 13, 38). Apoptotic cell death appears to be the primary mechanism for virus-induced tissue injury in the murine CNS (38, 39) and heart (11, 13).

In both cell culture models and the murine CNS, apoptosis induced by reovirus is contingent upon activation of transcription factor NF-κB (2, 8, 10, 39). NF-κB plays a critical role in the activation of innate immune responses (1, 45) and can either prevent or potentiate death signaling depending on the cell type and stimulatory cue (22). NF-κB family members exist as heterodimers or homodimers sequestered in the cytoplasm by association with IκBα or other structurally related inhibitors (1, 22). Agonists of NF-κB, including viral infection, trigger a signaling cascade that leads to phosphorylation and degradation of IκBα, which in turn permits translocation of NF-κB into the nucleus, where target gene transcription is activated (4).

Following reovirus infection, the prototypical form of NF-κB containing p50 and p65 subunits translocates to the nucleus and activates proapoptotic gene expression (10, 39). Activation of NF-κB is not dependent on viral RNA synthesis but does require signaling responses elicited by viral disassembly in the endocytic pathway (9). Reovirus-induced apoptosis is blocked in proteasome-arrested cells or following enforced cellular expression of degradation-resistant forms of IκBα, indicating that NF-κB is essential for proapoptotic signaling (10). Consistent with this requirement, cell lines deficient in either the p50 or p65 subunits of NF-κB are resistant to reovirus-induced apoptosis (10). Moreover, apoptosis is diminished in the CNS of mice lacking a functional *nfkb1*/*p50* gene (39).

Despite these data linking NF-κB to reovirus pathobiology, the underlying genetic program for reovirus-induced apoptosis is unknown. To identify the relevant NF-κB-responsive genes, we monitored gene expression profiles in mammalian cells that express a degradation-resistant mutant of IκBα (mIκBα) under the control of an inducible promoter (57). These microarray experiments revealed a network of NF-κB-regulated genes that are activated by reovirus in a temporal pattern. Remarkably, a substantial number of these transcription units are involved in host innate immune responses, including interferon

* Corresponding author. Mailing address: Lamb Center for Pediatric Research, D7235 MCN, Vanderbilt University School of Medicine, Nashville, TN 37232. Phone: (615) 343-9943. Fax: (615) 343-9723. E-mail: terry.dermody@vanderbilt.edu.

† Supplemental material for this article may be found at http://jvi.asm.org/.

‡ Present address: Department of Surgery, UCLA Medical Center, Los Angeles, CA 90095.

(IFN)-stimulated genes (ISGs). Our findings raise the possibility that innate immune response genes are involved in the mechanism by which NF-κB induces apoptosis in reovirus-infected cells.

MATERIALS AND METHODS

Cells and viruses. Spinner-adapted murine L929 (L) cells were grown in suspension or monolayer culture and maintained as described elsewhere (10). HeLa cells expressing mIκBα were generated and maintained as described previously (57). Expression of mIκBα was suppressed by the addition of 2 μg of doxycycline per ml to the medium. Reovirus strain type 3 Dearing (T3D) is a laboratory stock. Viral particles were purified by freon extraction of infected cell lysates and CsCl gradient centrifugation as described elsewhere (18). Titers of infectious virus were determined by plaque assay using L cell monolayers (61).

Immunoblot analysis. HeLa cells (7×10^6) grown in 100-mm tissue culture plates (Costar) were either induced to express mIκBα by doxycycline withdrawal or uninduced and either mock infected with phosphate-buffered saline or infected with reovirus T3D at a multiplicity of infection (MOI) of 100 PFU per cell. After viral adsorption at room temperature for 1 h, fresh medium was added, and cells were incubated at 37°C for 10 h. Nuclear and cytoplasmic extracts were prepared as described previously (10). Cytoplasmic extracts (50 μg of total protein) were electrophoresed in sodium dodecyl sulfate–10% polyacrylamide gels (29) and transferred to nitrocellulose membranes.

Immunoblotting was performed as previously described (42) using a rabbit polyclonal antiserum specific for IκBα (Santa Cruz Biotechnology), followed by horseradish peroxidase-conjugated goat anti-rabbit secondary antibody (Amersham Pharmacia Biotech), each diluted 1:1,000 in Tris-buffered saline containing 0.05% Tween 20 and 5% lowfat dry milk.

Electrophoretic mobility shift assays. HeLa cells (7×10^6) grown in 100-cm tissue culture plates were either induced or uninduced and adsorbed with reovirus T3D at an MOI of 100 PFU per cell. After incubation at 37°C for 0, 2, 6, and 10 h postinfection, cells were lysed in hypotonic lysis buffer (10 mM HEPES [pH 7.9], 10 mM KCl, 1.5 mM MgCl, 0.5 mM dithiothreitol, 0.5 mM phenylmethylsulfonyl fluoride, and protease inhibitor cocktail [Roche]) at 4°C for 15 min. A 1/20 volume of 10% Igepal CA-630 (Sigma Chemical Co.) was added to the cell lysate, and the sample was vortexed for 20 s and centrifuged at 12,000 × *g* for 5 min. The nuclear pellet was washed once in hypotonic buffer, resuspended in high-salt buffer (25% glycerol, 20 mM HEPES [pH 7.9], 0.42 M NaCl, 1.5 mM MgCl, 0.2 mM EDTA, 0.5 mM dithiothreitol, 0.5 mM phenylmethylsulfonyl fluoride, and protease inhibitor cocktail), and incubated at 4°C for 2 h. Samples were centrifuged at 12,000 × *g* for 10 min, and the supernatant was used as the nuclear extract.

Nuclear extracts (20 μg of total protein) were assayed for NF-κB activation by electrophoretic mobility shift assay using a ^{32}P-labeled oligonucleotide probe (1.0 ng) consisting of the NF-κB consensus binding sequence (Santa Cruz Biotechnology) as described elsewhere (10). Nucleoprotein complexes were subjected to electrophoresis in native polyacrylamide gels, which were dried and exposed to film.

Quantitation of reovirus growth. Induced or uninduced HeLa cells were grown in 24-well tissue culture plates (Costar) and infected with reovirus T3D at an MOI of 100 PFU per cell. After adsorption at room temperature for 1 h, 1.0 ml of fresh medium was added, and the cells were incubated at 37°C for 0, 12, 24, and 48 h. Following incubation, cells and culture medium were frozen (−70°C) and thawed twice, and viral titers in the cell lysates were determined by plaque assay using L cell monolayers (61).

Oligonucleotide probe-based microarrays. HeLa cells (7×10^6) grown in 100-cm tissue culture plates were either induced or uninduced and adsorbed with reovirus T3D at an MOI of 100 PFU per cell. After incubation at 37°C for 0, 2, 6, and 10 h postinfection, cells were lysed and RNA was extracted using TRIzol reagent according to the manufacturer's instructions (Invitrogen). Ten micrograms of total RNA was subjected to first-strand cDNA synthesis using a T7 RNA polymerase $(dT)_{24}$ oligomer (5′-GGCCAGTGAATTGTAATACGACTCACTATAGGGAGGCGG-dT_{24}-3′) and SuperScript II reverse transcriptase (Life Technologies). Bacteriophage T7 RNA polymerase was used to synthesize biotinylated cRNA according to the manufacturer's protocol (Enzo Diagnostics). The biotinylated target RNAs were fragmented to a mean size of 200 bases and hybridized to Hu95Av2 GeneChips (Affymetrix) containing 12,626 sequenced human genes according to the manufacturer's protocol. GeneChips were washed under both nonstringent (1 M NaCl, 25°C) and stringent (1 M NaCl, 50°C) conditions prior to staining with phycoerythrin-streptavidin (10 μg/ml final concentration). Arrays were scanned using a Gene Array scanner (Hewlett Packard) and analyzed using the GeneChip Analysis suite 5 software (Affymetrix). For each gene, 16 to 20 probe pairs were immobilized as ~25-mer oligonucleotides that hybridize throughout the mRNA; each probe pair was represented as a perfect match oligonucleotide and a mismatch oligonucleotide as a hybridization control. The "detection" of a given mRNA (i.e., whether the mRNA is detected ["present"] or not ["absent"]) and the "signal" (i.e., measure of mRNA abundance) were determined as previously described (31).

TABLE 1. Primers used for quantitative PCR

Primer	Sequence
IL-6 forward	5′-AAAGAGGCACTGGCAGAAAA-3′
IL-6 reverse	5′-TTTCACCAGGCAAGTCTCCT-3′
IRF-1 forward	5′-GCAGCTCAAAAAGGGAAGTG-3′
IRF-1 reverse	5′-AAGGCAGGAGTCATGCAAGT-3′
OAS1 (p40/46) forward	5′-CAAGCTCAAGAGCCTCATCC-3′
OAS1 (p40/46) reverse	5′-GAGCTCCAGGGCATACTGAG-3′
GAPDH forward	5′-CAACTACATGGTCTACATGTTC-3′
GAPDH reverse	5′-CTCGCTCCTGGAAGATG-3′

Data analysis. Two independent experiments were performed in which mRNA levels were compared by microarray analysis at 0, 2, 6, and 10 h following adsorption of induced and uninduced cells with either reovirus or gelatin saline as a mock infection control. For comparison of the fluorescence intensity (signal) values among multiple experiments, the signal values for each "experimental" GeneChip were scaled to those of the "base" GeneChip. This analysis was performed by first calculating the 2% trimmed mean (a measurement of global signal) for each GeneChip. The trimmed mean was obtained by calculating the mean signal of the chip after discarding the top and bottom 2% signal values (representing the "outliers"). Scaling was then performed by multiplying each of the signal measurements in the "experimental" array by a scaling factor defined as the ratio of the "base" trimmed mean to that of the "experimental" trimmed mean (the "base" array was defined to be the GeneChip for the zero-hour control mIκBα-induced cells). Because both reovirus infection and mIκBα induction (i.e., doxycycline withdrawal) can be considered experimental treatments, the scaled average difference values were subjected to a two-way analysis of variance with replications (ANOVA), as applied in the program Splus version 6 (Insightful), to identify genes that were significantly influenced by either reovirus infection or mIκBα induction.

Levels of gene expression were compared by hierarchical clustering following normalization of the average signal values by *Z*-score (57). The *Z*-score expresses the signal measurement of each gene during the course of treatment as a deviation from the mean in standard deviation units. For any cell, the *Z*-score is determined by the formula $Z = (S_i - S_{row})/SD$, where S_{row} is the average signal value for the gene (across the row) and SD is the standard deviation. Agglomerative hierarchical clustering was performed using the weighted pair-group method with arithmetic mean (Spotfire Array Explorer, version 8; Spotfire) using euclidean distance (5, 57).

Gene ontology analysis. Gene ontology analysis was performed using the functional annotation tool of the Database for Annotation, Visualization and Integrated Discovery (DAVID) 2.1 program (14). For each probe set, Gene Ontology:Biological Process (GO:BP) categories that were significantly overrepresented, as determined by the Fisher exact test ($P < 0.05$), were identified. The represented genes in GO:BP categories of interest were used for comparisons. For the reovirus-induced, NF-κB-dependent probe sets, identification of overrepresented GO:BP categories was verified using the NetAffx Analysis center (Affymetrix) (34).

Real-time PCR. RNA was extracted from 1×10^6 cells using TRIzol reagent. Three micrograms of RNA was used in a reverse transcription reaction mixture containing 10× buffer, 25 mM $MgCl_2$, 100 μM dithiothreitol, 1 U RNasin (Promega), 10 mM deoxynucleoside triphosphates, 50 μM random hexamers, and 1 U avian myeloblastosis virus) reverse transcriptase (Promega). The reaction mixture was incubated at 43°C for 1 h and terminated at 95°C for 10 min.

Real-time PCRs were performed using the Bio-Rad icycler and IQ supermix buffer containing DNA polymerase and SYBR Green (Bio-Rad). Two to three replicate amplification reactions were performed in 96-well plates (Bio-Rad). Each reaction mixture contained 12.5 μl IQ supermix buffer, 300 nM forward and reverse primers, and 1 μl cDNA in a final volume of 25 μl. Primers for the reactions are shown in Table 1. Cycling conditions were as follows: 95°C for 10 min and then 45 cycles at 95°C for 15 s, 60°C for 30 s, and 72°C for 15 s.

Data analysis was performed using the Bio-Rad icycler PCR detection and analysis software, version 3.0 (Bio-Rad). DNA was quantified using the standard curve method with the background subtracted. Known concentrations of

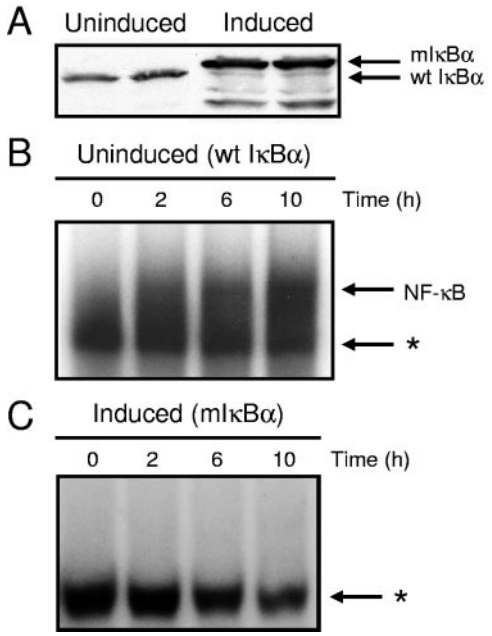

FIG. 1. IκBα expression and NF-κB activation in cells cultured in the presence and absence of doxycycline. (A) Expression of wt IκBα and mIκBα in the presence and absence of doxycycline. Cytoplasmic extracts were prepared at 7 days after either culture with doxycycline (uninduced) or doxycycline deprivation (induced). Extracts were subjected to immunoblotting using an IκBα-specific antiserum. (B and C) Time course of NF-κB gel shift activity in nuclear extracts prepared from reovirus-infected HeLa cells cultured in the presence (B) and absence (C) of doxycycline. Cells (5×10^6) were either uninduced or induced, infected with reovirus T3D at an MOI of 100 PFU per cell, and incubated at 37°C for the times shown. Nuclear extracts were prepared and incubated with a ^{32}P-labeled oligonucleotide consisting of the NF-κB consensus binding sequence. Incubation mixtures were resolved by acrylamide gel electrophoresis, dried, and exposed to film. NF-κB-containing complexes are indicated. *, nonspecific band.

cDNA were used to obtain the standard curve for each gene (concentrations between 0.0228 and 710 ng). A melting curve was determined for each sample to detect primer dimers, in which case data were not used. Results are expressed as the ratio of target cDNA and glyceraldehyde-3-phosphate dehydrogenase (GAPDH) cDNA.

RESULTS

NF-κB activation by reovirus is blocked in cells expressing mIκBα. To investigate whether NF-κB activation by reovirus is altered in cells induced to express mIκBα, we first confirmed the expression of mIκBα by doxycycline withdrawal. HeLa cells were cultured for 7 days in either the presence (uninduced) or absence (induced) of doxycycline. Cytoplasmic extracts were prepared and analyzed by immunoblotting for mIκBα and endogenous wild-type (wt) IκBα (Fig. 1A). Immunoblot analysis confirmed the expression of mIκBα following doxycycline withdrawal, indicating that these cells are appropriate for studies of NF-κB activation by reovirus. The difference in relative molecular mass exhibited by wt IκBα and mIκBα reflects a FLAG epitope tag appended to the carboxy terminus of mIκBα (57).

To determine whether expression of mIκBα is capable of blocking the NF-κB response elicited by reovirus, either uninduced or induced cells were infected with reovirus strain T3D, and nuclear extracts were prepared at 0, 2, 6, and 10 h postinfection. Extracts were incubated with a ^{32}P-labeled oligonucleotide probe consisting of an NF-κB consensus binding sequence and resolved in nondenaturing polyacrylamide gels (Fig. 1B and C). Following infection with reovirus, proteins capable of shifting the radiolabeled oligonucleotide to a higher relative molecular mass were increased in nuclear extracts prepared from uninduced cells (Fig. 1B) in comparison to extracts prepared from cells expressing mIκBα (Fig. 1C). NF-κB activation was first detected at 2 h postinfection and increased at 6 and 10 h postinfection in uninduced cells (Fig. 1B). In contrast, little NF-κB activation was detected at any time point in cells induced to express mIκBα (Fig. 1C). These results demonstrate that reovirus stimulates nuclear translocation of NF-κB complexes in uninduced cells but not in cells expressing mIκBα.

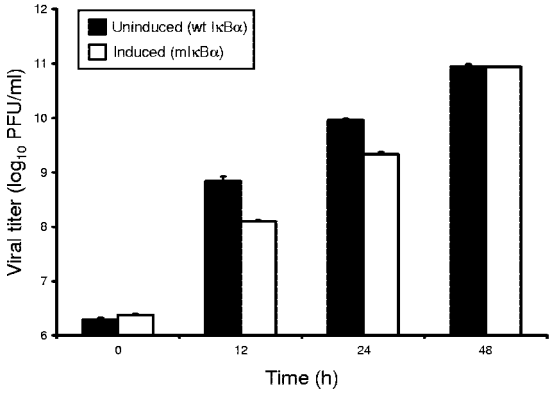

FIG. 2. Growth of reovirus in HeLa cells cultured in the presence and absence of doxycycline. HeLa cells (1×10^5) were either uninduced or induced, infected with reovirus T3D at an MOI of 100 PFU per cell, and incubated at 37°C for the times shown. Viral titers were determined by plaque assay using L cells. The results are presented as the mean viral titers for three independent experiments. Error bars indicate standard deviations.

To determine whether the absence of NF-κB activation in HeLa cells expressing mIκBα is due to a failure of reovirus to productively infect these cells, uninduced and induced HeLa cells were infected with reovirus T3D, and viral titers were determined by plaque assay at 0, 12, 24, and 48 h postinfection (Fig. 2). Reovirus replicated efficiently in both uninduced and induced cells, although yields of progeny virus were greater in uninduced cells at 12 and 24 h of infection. By 48 h, viral yields in uninduced and induced cells were equivalent. Together with results presented in Fig. 1, these data indicate that mIκBα potently blocks NF-κB signaling in cells but does not abolish viral replication, validating the use of mIκBα-expressing cells for studies to assign NF-κB gene targets.

Identification of an NF-κB-dependent gene network in reovirus-infected cells. To identify gene expression profiles dependent on reovirus infection and NF-κB activation, mIκBα-expressing HeLa cells were cultured in the presence or absence of doxycycline for 7 days prior to infection with reovirus T3D. RNA was harvested from duplicate samples of mock-infected and reovirus-infected cells at 0, 2, 6, and 10 h postinfection (Fig. 1B). Gene expression changes were detected by using high-density oligonucleotide microarrays containing oligonucleotides corresponding to approximately 12,696 sequenced hu-

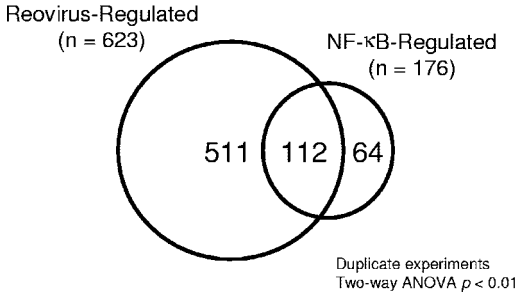

FIG. 3. Cellular genes regulated by reovirus and NF-κB. Two-way ANOVA of scaled signal intensities was used to identify genes regulated by either reovirus infection or mIκBα expression. Probe sets with a P value of <0.01 by either treatment were selected for further analysis. Shown is a Venn diagram of genes common to both data sets. Of the 623 genes regulated by reovirus, 112 also are under NF-κB control.

man genes (Affymetrix Hu95A GeneChip). Two-way ANOVA was used to identify changes in expression levels that were significantly altered ($P < 0.01$) following reovirus infection. In these experiments, reovirus infection significantly influenced the expression of 623 mRNAs represented on the GeneChip (Fig. 3). Induction of mIκBα significantly changed the expression of 176 mRNAs. Comparison of the two expression profile groups revealed that there were 112 genes common to both reovirus infection and NF-κB activation (Fig. 3 and Table 2). Since the expression of these 112 genes is dependent on both reovirus and NF-κB, these genes were chosen for further analysis.

Identification of distinct expression patterns of NF-κB-regulated genes in response to reovirus infection. To characterize gene expression profiles that are dependent on both reovirus infection and NF-κB activation and to determine whether NF-κB gene expression is temporally regulated during reovirus infection, we used a hierarchical clustering algorithm to define the relationship of genes of interest (64). Each gene expression profile was grouped with its nearest neighbor, and the mathematical proximity of each expression profile to that of the others was defined. The hierarchical clustering of 112 genes with expression patterns dependent on both reovirus and NF-κB is shown in Fig. 4, with the data visually presented using a color-coded scale. Inspection of the dendrogram reveals four distinct gene clusters with expression patterns that are dependent on the time of infection. The second, third, and fourth clusters include genes that are induced by reovirus and blocked by expression of mIκBα. In general, genes in cluster III were maximally expressed 2 h postinfection (kinetic class 1), genes in cluster IV were expressed 6 h postinfection (kinetic class 2), and genes in cluster II were expressed 10 h postinfection (kinetic class 3). Cluster I includes genes with low-level expression in uninduced cells that are enhanced by expression of mIκBα. These genes appear to be constitutively regulated by NF-κB. We conclude that distinct groups of NF-κB-dependent genes are induced by reovirus at distinct times during infection.

NF-κB-regulated genes induced by reovirus belong to distinct functional classes. To determine whether reovirus-responsive genes under NF-κB control can be grouped into functional classes, we used the functional annotation tool of the DAVID program. Biological processes in each kinetic class that were statistically overrepresented by the Fisher exact test ($P < 0.05$) were identified. Biological processes overrepresented in kinetic class 1 include cell proliferation, taxis, apoptosis, and response to pest, pathogen, or parasite. Taxis and response to pest, pathogen, or parasite also were represented in kinetic class 3, along with the Janus-activated kinase (JAK) signal transducer and activator of transcription (STAT) cascade and response to virus. No overrepresented biological processes were identified in kinetic class 2. Thus, distinct classes of genes under NF-κB control are activated following reovirus infection.

Confirmation of microarray analysis by real-time PCR. To confirm the temporal expression pattern of NF-κB-responsive genes identified in the microarray analysis, we used real-time PCR to define the expression levels of single genes during the interval of reovirus infection employed in the microarray experiments. Either uninduced or induced HeLa cells were infected with reovirus T3D, and RNA was harvested at 0, 2, 6, and 10 h postinfection. Following reverse transcription, resultant cDNAs were used in real-time PCRs to detect levels of interleukin-6 (IL-6), IRF-1, and p40/46 OAS1 mRNA (Fig. 5). The results demonstrated that these genes are upregulated following reovirus infection in an NF-κB-dependent manner with kinetics that parallel the microarray results.

DISCUSSION

Apoptotic cell death is the primary mechanism of reovirus-induced tissue injury in the murine CNS (38, 39) and heart (11, 13). Emerging mechanistic evidence indicates that transcription factor NF-κB plays an important role in the present death response (2, 8, 10, 39). However, until the present study, the underlying genetic program elicited by NF-κB activation in reovirus-infected cells remained unknown. To identify the relevant NF-κB-responsive genes, we monitored gene expression profiles in mammalian cells engineered to express a degradation-resistant mutant of IκBα (57). NF-κB-dependent alterations in the expression of 112 genes were observed following reovirus infection. This set of genes includes several members that have been linked to apoptosis, including STAT1, GADD45A, and RhoB (32, 46, 58).

Our gene profiling studies revealed a wide spectrum of reovirus-inducible genes under NF-κB control, including those encoding cytokines, transcription factors, cell cycle regulators, and enzymes (Table 2). Cytokine and cell proliferation genes were expressed at 2 h postinfection, NF-κB family members were expressed at 6 h postinfection, and ISGs were expressed at 10 h postinfection. These findings suggest that distinct gene clusters are temporally regulated following infection with reovirus. Genes encoding cytokines (e.g., IL-6, IL-8, CXCL1/GROα, and CXCL2/MIP-2α) were among the most rapidly expressed, which likely reflects their involvement in the activation of downstream signaling pathways for innate immunity. Thus, some of the NF-κB response genes identified in our study may be secondarily dependent on signaling pathways triggered by cytokines secreted early in the reovirus infectious cycle.

Innate immunity plays an important role in host defense by limiting viral replication and facilitating development of an adaptive immune response (4). Modification of the NF-κB

TABLE 2. Expression profiles of reovirus-regulated genes[a]

Cluster and gene symbol	GenBank accession no.	Mean scaled avg difference								Pr(F)	
		NF-κB intact (+Dox)				NF-κB inhibited (−Dox)				NF-κB (+Dox)	Reovirus
		0 h	2 h	6 h	10 h	0 h	2 h	6 h	10 h		
Cluster I											
POLD1	M80397	80	67	67	62	802	73	69	77	4.81E-08	5.73E-09
CGA	S70585	6,909	8,097	6,852	6,705	8,215	9,129	8,553	8,277	6.00E-07	1.43E-04
MFAP2	U19718	4,730	4,359	3,853	3,466	6,048	5,222	4,759	4,718	7.00E-07	1.10E-05
SLC9A8	AL031685	80	67	67	62	233	73	69	77	1.65E-05	2.46E-06
HR	W27191	80	67	67	62	269	73	69	77	1.94E-05	2.86E-06
BAPX1	AF009801	352	227	269	243	438	311	342	396	9.46E-05	1.30E-03
ERCC4	L76568	80	67	67	62	76	304	69	77	4.93E-04	1.74E-04
POU6F1	Z21966	80	67	67	62	93	165	69	77	1.02E-03	2.39E-03
LMO1	M26682	554	309	335	384	916	390	419	481	1.09E-03	8.32E-05
INSIG1	U96876	373	372	184	190	558	484	184	333	1.11E-03	5.14E-05
RAB5B	X54871	479	394	353	342	564	487	395	507	1.46E-03	5.88E-03
ARL3	AF038193	80	67	67	62	179	73	69	77	1.83E-03	4.41E-04
HBP1	AF019214	299	265	124	186	419	283	148	189	2.17E-03	6.93E-07
PPP1R3C	N36638	242	308	228	184	334	474	263	244	2.18E-03	1.22E-03
ACADS	Z80345	80	67	67	62	234	73	106	77	2.37E-03	2.96E-03
CLK3	L29217	388	282	262	283	354	290	69	242	2.85E-03	1.00E-04
RABGGTA	Y08200	389	365	380	404	405	373	69	372	2.99E-03	6.17E-04
IL10RB	AI984234	458	404	408	397	643	537	415	450	3.06E-03	9.20E-03
FOS	V01512	928	1,283	778	156	1,018	1,972	853	263	3.12E-03	1.02E-06
MTUS1	AL096842	392	310	268	315	513	419	291	392	6.13E-03	4.27E-03
ARMC6	AC003038	697	675	67	62	330	73	69	77	6.65E-03	2.70E-03
SMAD2	U68018	671	852	688	735	814	962	702	851	7.99E-03	3.14E-03
LAMA4	S78569	118	97	79	79	176	134	98	98	8.02E-03	7.02E-03
CLDN7	AJ011497	245	185	146	152	286	225	180	229	8.11E-03	4.25E-03
DDR1	L20817	381	378	330	248	477	445	294	341	8.37E-03	5.99E-04
HTRA1	D87258	1,510	1,404	1,194	950	1,776	1,822	1,289	1,369	9.24E-03	8.39E-03
NOTCH3	U97669	708	474	383	320	815	692	417	463	9.53E-03	3.03E-04
CHES1	U68723	364	301	308	330	508	355	319	383	9.54E-03	8.58E-03
HYAL1	U03056	370	224	148	124	443	243	133	181	9.90E-03	2.10E-07
Cluster II (kinetic class 3)											
IRF1	L05072	80	67	619	664	76	73	69	77	8.10E-11	7.18E-10
OAS1 (p40/46)	X04371	80	67	67	846	76	73	69	77	1.76E-10	1.69E-11
TNIP1	AJ011896	80	67	1,138	1,290	76	73	69	77	9.47E-08	8.07E-07
G1P2	AA203213	79.5	194	661	3,472	76	73	553	1,620	3.03E-07	1.79E-11
CCL5	M21121	80	67	267	692	76	73	69	225	2.45E-06	1.46E-07
IRF7	U53831	80	67	67	631	76	73	69	183	3.88E-06	1.88E-08
G1P3	U22970	80	67	67	1,260	76	73	69	406	5.97E-06	7.80E-09
STAT1	M97936	261	265	391	1,457	301	264	303	443	1.75E-05	1.75E-06
MX2	M30818	80	67	67	236	76	73	69	75	4.15E-05	3.44E-06
IFIT1	M24594	110	98	1,090	7,793	99	99	864	3,164	6.20E-05	2.59E-08
STAT2	U18671	80	67	67	219	76	73	69	77	6.92E-05	4.37E-06
OGFR	AF109134	1,545	1,636	1,543	3,024	1,385	1,329	1,140	1,485	1.09E-04	2.43E-04
FXYD2	H94881	80	67	67	62	76	73	69	187	1.26E-04	8.51E-05
CXCL10	X02530	80	67	62	226	76	73	69	77	1.54E-04	7.62E-06
EBNA1BP2	U86602	2,599	2,573	2,757	3,066	2,216	2,306	2,384	2,536	1.56E-04	5.24E-03
PLSCR1	AB006746	719	781	1,142	3,321	715	718	697	1,024	1.61E-04	2.75E-05
CXCL11	AF030514	80	67	90	437	76	73	69	80	1.92E-04	3.65E-05
BF	L15702	80	67	365	415	76	73	69	77	3.28E-04	2.40E-03
IFIT5	U34605	140	163	206	452	162	134	181	229	3.53E-04	4.08E-06
OASL (p59)	AJ225089	80	237	2,092	11,230	76	148	1,646	6,298	5.01E-04	1.82E-08
NMI	U32849	578	446	497	954	495	468	388	504	6.54E-04	3.80E-04
SP110	L22342	80	67	67	413	76	73	69	77	8.88E-04	1.21E-04
TDRD7	AB025254	80	67	99	396	76	73	69	121	9.74E-04	4.87E-05
FLJ38348	AL047596	208	217	323	817	261	230	265	352	1.87E-03	2.16E-05
TAP1	X57522	434	332	554	916	316	290	406	415	1.93E-03	2.42E-03
IFITM1	J04164	1,730	1,477	1,376	4,210	1,641	1,524	1,202	1,451	2.31E-03	8.63E-04
TUBB4	U47634	3,747	3,720	3,899	4,407	2,979	3,247	3,409	3,942	2.69E-03	9.33E-03
PML	M82827	174	67	163	817	76	73	69	77	2.80E-03	4.24E-03
PODXL	U97519	887	881	1,224	1,259	805	752	987	1,019	3.29E-03	8.79E-04
IL15	AF031167	148	138	274	330	168	144	212	155	3.84E-03	7.45E-04
PTGES	AF010316	427	879	1,145	1,148	76	73	846	1,060	4.30E-03	7.21E-04
TRIM21	M62800	160	176	231	795	223	174	115	231	4.83E-03	7.46E-04

Continued on facing page

TABLE 2—*Continued*

Cluster and gene symbol	GenBank accession no.	Mean scaled avg difference								Pr(F)	
		NF-κB intact (+Dox)				NF-κB inhibited (−Dox)				NF-κB (+Dox)	Reovirus
		0 h	2 h	6 h	10 h	0 h	2 h	6 h	10 h		
RAD51C	AF029669	307	205	234	179	262	164	144	176	6.85E-03	8.24E-04
IFI16	M63838	618	469	417	1,565	517	504	370	524	7.21E-03	1.97E-03
HEG1	W28612	861	949	1,452	1,690	732	956	1,143	1,173	7.66E-03	5.03E-04
IFIT2	M14660	80	67	562	4,647	76	73	681	2,518	7.73E-03	2.97E-07
DPH2	AF053003	964	1,061	1,201	1,229	912	929	1,127	1,079	8.63E-03	1.22E-03
GSTM3	J05459	458	340	418	348	345	73	423	384	8.90E-03	1.04E-03
ANXA3	M20560	311	352	546	683	205	233	447	475	9.01E-03	9.48E-04
LHFPL2	D86961	522	414	553	582	591	474	576	615	9.30E-03	2.10E-04
UBC	AB009010	4,699	4,354	4,769	5,500	5,370	4,746	5,423	5,881	9.33E-03	5.68E-03
IFI44	D28915	170	211	758	2,453	156	162	618	1,452	9.84E-03	1.81E-06
Cluster III (kinetic class 1)											
IL6	X04430	80	1,222	1,116	759	76	355	235	180	2.44E-08	3.85E-07
CXCL2	M36820	46	395	205	204	76	139	105	79	5.01E-07	5.68E-07
PLK3	U56998	80	869	67	62	76	73	69	77	1.35E-06	1.41E-07
TNFAIP3	M59465	132	742	588	380	91	350	190	183	7.00E-06	1.25E-05
PSMB9	AA808961	370	318	321	646	268	218	221	199	1.47E-05	1.99E-03
NFKBIA	M69043	706	2,079	1,664	1,126	717	1,340	953	627	1.04E-04	2.77E-05
IL8	M28130	80	1,866	580	62	76	421	69	77	2.61E-04	3.12E-05
CXCL1	X54489	117	615	341	162	76	351	69	77	3.67E-04	3.71E-05
GADD45A	M60974	362	687	563	430	392	538	422	398	3.93E-04	4.73E-06
NFKB1	M58603	2,747	3,708	4,029	3,044	2,836	2,802	2,908	2,515	5.40E-04	5.02E-03
IFNGR1	U19247	297	479	480	362	282	372	321	234	5.83E-04	1.48E-03
CCND1	M64349	1,097	1,339	1,452	917	1,009	1,106	946	800	5.89E-04	1.17E-03
PLK2	AF059617	68	736	382	185	76	419	198	125	7.35E-04	3.84E-06
IFITM3	X57352	9,310	9,027	8,522	15,241	7,661	6,352	7,720	8,288	9.43E-04	4.63E-03
TNFAIP2	M92357	1,029	1,560	1,619	880	943	1,252	1,028	822	1.11E-03	1.90E-04
PLAUR	U09937	1,112	2,347	1,785	2,146	1,028	2,106	1,644	1,529	1.74E-03	5.26E-06
JUNB	M29039	573	1,466	1,031	772	589	1,175	918	456	1.94E-03	2.68E-06
IL4R	X52425	168	365	360	192	148	274	224	100	2.47E-03	3.57E-04
TNFAIP8	AF099935	526	729	675	534	553	625	479	502	2.65E-03	9.96E-04
RND3	S82240	282	677	427	489	244	583	309	348	3.55E-03	3.15E-05
PTPN1	M93425	740	1,183	843	664	682	1,016	560	562	4.09E-03	8.53E-05
EPHA2	M59371	300	1,192	810	329	248	886	511	193	4.50E-03	1.26E-05
PSCD1	M85169	243	483	344	244	198	402	196	262	5.93E-03	7.12E-05
IER3	S81914	568	1,976	847	448	621	1,569	584	385	6.79E-03	1.40E-07
ID1	X77956	5,708	15,703	10,646	8,703	5,801	14,940	9,909	6,742	7.40E-03	1.00E-08
BCAR3	U92715	295	726	587	303	239	686	370	270	8.29E-03	4.96E-06
AMIGO2	AC004010	172	698	483	286	152	633	385	237	8.84E-03	1.00E-07
CEBPD	M83667	577	1,440	903	931	557	1,202	611	660	8.89E-03	1.18E-04
Cluster IV (kinetic class 2)											
PLAU	X02419	296	902	1,034	586	254	707	705	412	1.06E-06	5.40E-09
NFKB2	U20816	80	306	431	328	76	73	69	77	1.74E-06	6.60E-04
RHOB	M12174	652	1,257	1,242	1,605	903	1,522	1,957	1,839	3.65E-05	1.80E-06
RELB	M83221	80	421	623	422	76	203	69	77	1.23E-04	6.86E-03
SDC4	D79206	169	524	672	503	202	431	353	251	5.10E-04	1.53E-04
MAFF	AL021977	80	370	131	65	76	187	79	77	9.11E-04	2.80E-06
TRIM16	AF096870	729	1,163	1,908	1,686	767	832	1,161	1,022	3.43E-03	2.80E-03
GALNT1	U41514	355	418	444	424	333	359	365	403	3.57E-03	9.82E-03
OSMR	U60805	323	540	597	552	340	473	481	362	3.89E-03	8.06E-04
JUN	J04111	116	182	171	140	89	250	209	157	4.13E-03	4.81E-06
TXNRD1	X91247	3,421	4,352	5,620	4,496	3,151	4,230	4,786	3,948	4.67E-03	2.00E-05
BIRC2	U37547	251	443	548	474	249	392	391	359	7.50E-03	7.38E-04
NPR3	M59305	586	787	861	835	744	832	885	973	8.85E-03	1.00E-03

[a] Shown are reovirus-responsive, NF-κB-dependent genes identified in the microarray analysis, categorized by gene cluster and kinetic class. The gene symbol, GenBank accession number, mean scaled average difference values for each treatment condition, and the *P* value [Pr(F)] as a function of either NF-κB signaling or reovirus infection are shown for each gene identified. Dox, doxycycline. Within each cluster, genes are listed according to statistical significance for NF-κB dependence.

signaling pathway by viruses is a common mechanism to enhance viral replication, manipulate host immunity, influence cell growth, and determine cell fate (1, 25). Following viral infection, NF-κB activation elicits innate immune responses by the production of IFN-α/β, which function as potent antiviral cytokines (44). Secreted IFN-α/β act in a paracrine manner to produce an antiviral state in uninfected cells through activation of the JAK-STAT signal transduction pathway (44). Based on

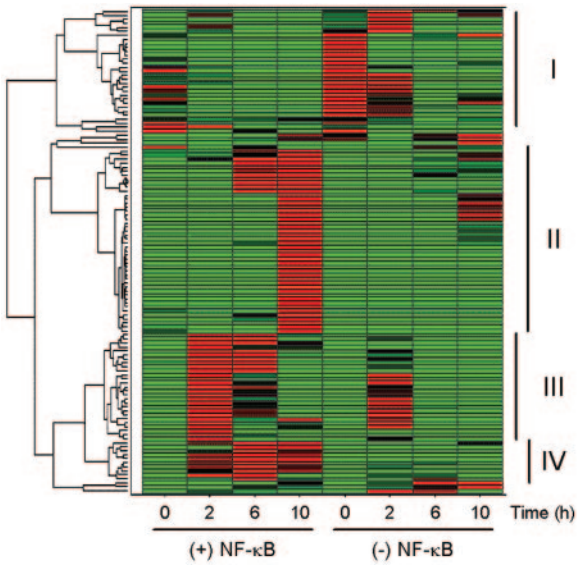

FIG. 4. Hierarchical clustering of mRNA expression profiles. The signal intensities of probe sets were normalized by *Z*-score and subjected to hierarchical clustering. Data are represented as a heat map, where each row represents a different probe set. At each time point, the calculated *Z*-score is shown by a color code in which red represents a Z of $>+1.2$, green represents a *Z* of <-1.2, and black represents a *Z* of 0. The treatment conditions are indicated at the bottom of the figure. Shown at the left is a dendrogram indicating the mathematical relationship of the expression profiles. Genes with similar expression profiles are grouped together and connected by a short line that connects the two nodes. Four major clusters are evident, labeled I to IV, at the right.

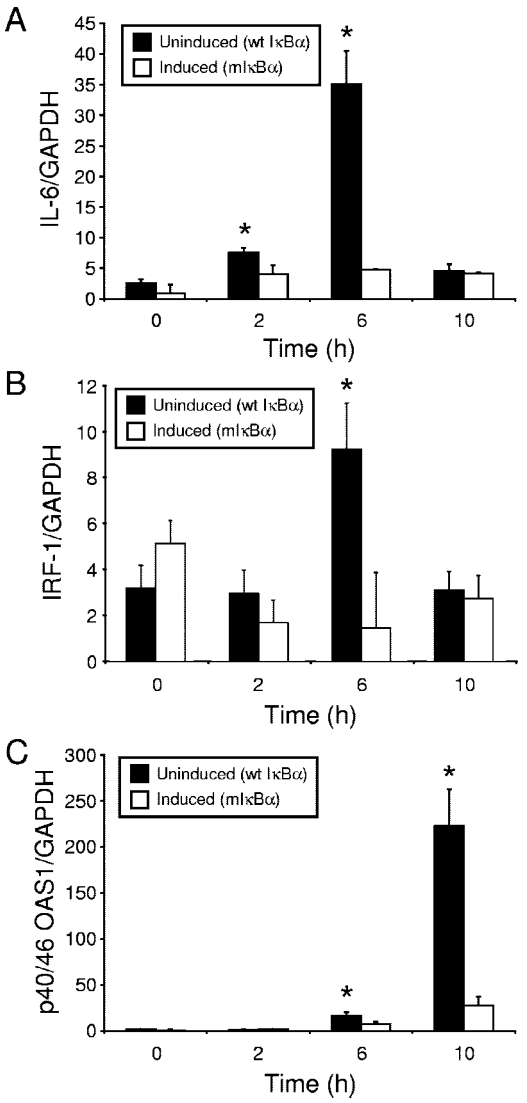

FIG. 5. Levels of mRNAs corresponding to reovirus-responsive, NF-κB-dependent genes in cells expressing mIκBα and cells expressing wild-type IκBα. HeLa cells were either uninduced or induced and infected with reovirus T3D at an MOI of 100 PFU per cell. At 0, 2, 6, and 10 h postinfection, RNA was extracted and used as a template to generate cDNA. Levels of (A) IL-6, (B) IRF-1, (C) p40/46 OAS1, and GAPDH mRNA were quantified by real-time PCR. The results are expressed as a ratio of target cDNA to GAPDH cDNA. Shown are the mean ratios of two independent experiments performed in duplicate. Error bars indicate standard deviations. *, $P < 0.05$ by *t* test in comparison to induced cells at each time point.

the microarray data in this report, indicating that ISGs are induced in an NF-κB-dependent fashion following reovirus infection, we conclude that reovirus-induced activation of NF-κB has potent stimulatory effects on mechanisms of innate immunity.

Many of the biological effects of IFN-α/β and other IFNs are mediated by ISGs (48), which have been previously implicated in cell death signaling (24). STAT-1 is activated upon IFN binding to its receptor, and it forms a complex with STAT-2/p48 (ISGF3) to induce transcription (26). IFN regulatory factor 1 (IRF-1) is a target for STAT-1 transcriptional regulation (41), and IRF-1 itself transcriptionally regulates additional ISGs and promotes apoptosis following DNA damage (23, 51, 53). IFN-α/β can greatly enhance the apoptotic response of cultured cells to double-stranded RNA and influenza virus (54). In this regard, Tanaka et al. (54) have proposed that only virus-infected cells producing IFN undergo apoptosis following viral infection (54). According to this model, IFN induces cytotoxicity of infected cells via an autocrine pathway, whereas uninfected cells enter an antiviral state via a paracrine mode of IFN action (54). Of note, we found that NF-κB activation by reovirus leads to expression of STAT-1, STAT-2, and IRF-1 (Tables 2 and 3). This finding raises the possibility that reovirus induces apoptosis as a consequence of NF-κB-mediated stimulation of ISGs.

In addition to the NF-κB-dependent innate immune response, reovirus infection induces expression of genes in other proapoptotic pathways, through both NF-κB-dependent (e.g., GADD45A [58] and RhoB [33]) and NF-κB-independent (e.g., TP53BP2/ASPP2 and PPP1R13B/ASPP1 [43]) mechanisms. GADD45A, RhoB, TP53BP2, and PPP1R13B have been implicated in the cellular response to DNA damage initiated by the p53 tumor suppressor (28, 35, 47). It is noteworthy that genes in the DNA damage response pathway are overrepresented among reovirus-regulated genes identified in this and a previous microarray study (12). DNA damage response genes identified in both studies include GADD45A, DDB2, ERCC4, FUS, and IRF-7. The pathological relationship between reovirus infection, NF-κB activation, and the

TABLE 3. Host defense response genes induced by reovirus[a]

Class and gene symbol	GenBank accession no.	Avg fold increase			
		0 h	2 h	6 h	10 h
Kinetic class 1					
CXCL1	X54489	1.54	1.75	4.98	2.10
CXCL2	M36820	0.61	2.84	1.96	2.57
IFITM3	X57352	1.22	1.42	1.1	1.84
IL4R	X52425	1.14	1.33	1.60	1.91
IL6	X04430	1.05	3.45	4.75	4.21
IL8	M28130	1.05	4.43	8.46	0.80
NFKB1	M58603	0.97	1.32	1.38	1.21
Kinetic class 3					
PSMB9	AA808961	1.38	1.46	1.45	3.24
BF	L15702	1.04	0.91	5.35	5.38
CCL5	M21121	1.04	0.91	3.92	3.07
CXCL10	X02530	1.05	0.91	0.91	2.93
CXCL11	AF030514	1.05	0.91	1.31	5.45
G1P2	AA203213	1.05	2.65	1.2	2.14
G1P3	U22970	1.05	0.91	0.98	3.11
IFI16	M63838	1.2	0.93	1.13	2.99
IFIT1	M24594	1.78	1.04	1.1	3.14
IFIT2	M14660	1.05	0.91	0.83	1.85
IFIT5	U34605	0.86	1.22	1.13	1.97
IFITM1	J04164	1.05	0.97	1.14	2.90
IL15	AF031167	0.87	0.95	1.29	2.12
IRF1	L05072	1.05	0.91	9.04	8.62
IRF7	U53831	1.05	0.91	0.98	3.44
MX2	M30818	1.05	0.91	0.98	3.15
NMI	U32849	1.17	0.91	1.28	1.89
OAS1 p40/46	X04371	1.05	0.91	0.98	10.98
OASL p59	AJ225089	1.05	1.6	1.27	1.78
PTGES	AF010316	5.6	12.02	1.35	1.08
TAP1	X57522	1.37	1.14	1.36	2.21

[a] Shown is a subset of reovirus-responsive, NF-κB-dependent genes identified in the microarray analysis that are categorized as defense response by the DAVID program (14). Genes are listed alphabetically by kinetic class. Average fold change is expressed as a ratio of mRNA levels in uninduced cells (+doxycycline) divided by mRNA levels in induced cells (−doxycycline) at the indicated times after infection. Values less than 1 represent a decrease in expression.

cellular response to DNA damage, if any, remains unclear. However, there is evidence for significant interactions between the NF-κB and p53 pathways (15, 63), which may be operative in reovirus-infected cells. In support of this possibility, we identified two NF-κB-responsive genes in kinetic class 1 that have been previously implicated in the regulation of p53-mediated apoptosis (PLK3 and IER3/IEX-1) (30). In addition to regulating genes in the p53-mediated apoptotic pathway, reovirus infection regulates several genes involved in mitochondrial injury pathways, including MCL1 (3), PAWR/Par-4 (21), BNIP3L (27), and MOAP1 (52). However, NF-κB is not required for the regulation of these genes by reovirus, suggesting that these genes may function in concert with certain NF-κB-responsive genes to modulate the apoptotic response in reovirus-infected cells.

In prior studies, we observed decreased yields of reovirus following growth in cells lacking either the p50 or p65 NF-κB subunits in comparison to wt controls (10). Yields of reovirus in cells induced to express mIκBα were also lower than those in uninduced cells following 12 and 24 h of viral growth. Reovirus produces substantially greater yields following growth in rapidly dividing or transformed cells (16, 49, 55), suggesting that cellular factors associated with cell growth augment viral replication. It is possible that a subset of NF-κB-regulated genes promotes cell proliferation, which in turn enhances viral nucleic acid or protein synthesis, intracellular transport of viral proteins, or assembly and release of progeny virions. These genes include those that encode cell cycle proteins, such as PLK2 (36), and cytokines, such as CXCL1, CXCL10, IL-6, and IL-8.

NF-κB-dependent gene networks that are activated in response to a variety of other stimuli have been described, including respiratory syncytial virus (57), Epstein-Barr virus (6), tumor necrosis factor alpha (56), and heart disease (20). Gene ontology analysis of these data reveal significant representation of genes involved in cellular proliferation, apoptosis, signal transduction, taxis, and host defense responses (see Table S1 in the supplemental material). For example, upregulation of CCL5/RANTES, NFKBIA/IκBα, NFKB2/p49/p100, and TNFAIP3/A20 was observed in four of five studies, including this study, while NFKB1/p50/p105, CXCL1/GRO-α, IL-6, and IL-8 were observed in three of five studies. Several genes, including those encoding retinoic acid receptor-α, glomulin, and placental growth factor, were classified as NF-κB dependent in one study (57) but not in this study. These divergent results suggest that such genes can be differentially regulated via agonist-specific mechanisms. Alternatively, a requirement for NF-κB may be a function of the interval following stimulation or the cell type. The expression of NF-κB-dependent genes, including CCL5, IL-6, and TNFAIP3, in failing human hearts is of particular significance (20), as we have recently shown that NF-κB activation protects the heart from reovirus-induced apoptosis in vivo (39). It will therefore be of interest to examine the expression of these genes in the heart of neonatal mice during infection with myocarditic and nonmyocarditic reovirus strains.

NF-κB plays an essential role in the genetic response to a variety of cellular stresses (19). The extensive array of NF-κB inducers and target genes suggests that numerous mechanisms exist to direct transcription of appropriate NF-κB-responsive genes due to specific stimuli (40). Here, we have identified a network of genes activated by NF-κB following reovirus infection. Many of these genes function in innate immunity (Table 3), suggesting a critical role for this component of host defense in proapoptotic signaling. These genes may act in concert with genes involved in other proapoptotic pathways that reovirus regulates, including the DNA damage response and mitochondrial injury pathways. Data presented in this report establish the requisite genetic framework to address this potential interplay and to further dissect the pathological mechanisms of reovirus-induced apoptosis.

ACKNOWLEDGMENTS

We thank Jim Chappell, Pranav Danthi, and Mark Hansberger for careful review of the manuscript and Shawn Levy for assistance in the design of the microarray experiments.

This research was supported by Public Health Service awards T32 AI07474 (S.M.O.), T32 AI49824 (G.H.H.), R01 AI052379 (D.W.B), R01 AI50080 (T.S.D), the Vanderbilt University Medical Scholars Program (M.J.W.), and the Elizabeth B. Lamb Center for Pediatric Research. Additional support was provided by Public Health Service awards CA68485 for the Vanderbilt-Ingram Cancer Center and DK20593 for the Vanderbilt Diabetes Research and Training Center.

REFERENCES

1. **Baldwin, A. S., Jr.** 2001. The transcription factor NF-κB and human disease. J. Clin. Investig. **107:**3–6.

2. **Barton, E. S., J. C. Forrest, J. L. Connolly, J. D. Chappell, Y. Liu, F. Schnell, A. Nusrat, C. A. Parkos, and T. S. Dermody.** 2001. Junction adhesion molecule is a receptor for reovirus. Cell **104:**441–451.
3. **Bingle, C. D., R. W. Craig, B. M. Swales, V. Singleton, P. Zhou, and M. K. B. Whyte.** 2000. Exon skipping in Mcl-1 results in a Bcl-2 homology domain 3 only gene product that promotes cell death. J. Biol. Chem. **275:**22136–22146.
4. **Bose, S., and A. K. Banerjee.** 2003. Innate immune response against nonsegmented negative strand RNA viruses. J. Interferon Cytokine Res. **23:**401–412.
5. **Brasier, A. R., H. Spratt, Z. Wu, I. Boldogh, Y. Zhang, R. P. Garofalo, A. Casola, J. Pashmi, A. Haag, B. Luxon, and A. Kurosky.** 2004. Nuclear heat shock response and novel nuclear domain 10 reorganization in respiratory syncytial virus-infected A549 cells identified by high-resolution two-dimensional gel electrophoresis. J. Virol. **78:**11461–11476.
6. **Cahir-McFarland, E. D., K. Carter, A. Rosenwald, J. M. Giltnane, S. E. Henrickson, L. M. Staudt, and E. Kieff.** 2004. Role of NF-κB in cell survival and transcription of latent membrane protein 1-expressing or Epstein-Barr virus latency III-infected cells. J. Virol. **78:**4108–4119.
7. **Chappell, J. D., J. L. Duong, B. W. Wright, and T. S. Dermody.** 2000. Identification of carbohydrate-binding domains in the attachment proteins of type 1 and type 3 reoviruses. J. Virol. **74:**8472–8479.
8. **Connolly, J. L., E. S. Barton, and T. S. Dermody.** 2001. Reovirus binding to cell surface sialic acid potentiates virus-induced apoptosis. J. Virol. **75:**4029–4039.
9. **Connolly, J. L., and T. S. Dermody.** 2002. Virion disassembly is required for apoptosis induced by reovirus. J. Virol. **76:**1632–1641.
10. **Connolly, J. L., S. E. Rodgers, P. Clarke, D. W. Ballard, L. D. Kerr, K. L. Tyler, and T. S. Dermody.** 2000. Reovirus-induced apoptosis requires activation of transcription factor NF-κB. J. Virol. **74:**2981–2989.
11. **DeBiasi, R., C. Edelstein, B. Sherry, and K. Tyler.** 2001. Calpain inhibition protects against virus-induced apoptotic myocardial injury. J. Virol. **75:**351–361.
12. **DeBiasi, R. L., P. Clarke, S. Meintzer, R. Jotte, B. K. Kleinschmidt-Demasters, G. L. Johnson, and K. L. Tyler.** 2003. Reovirus-induced alteration in expression of apoptosis and DNA repair genes with potential roles in viral pathogenesis. J. Virol. **77:**8934–8947.
13. **DeBiasi, R. L., B. A. Robinson, B. Sherry, R. Bouchard, R. D. Brown, M. Rizeq, C. Long, and K. L. Tyler.** 2004. Caspase inhibition protects against reovirus-induced myocardial injury in vitro and in vivo. J. Virol. **78:**11040–11050.
14. **Dennis, G., Jr., B. T. Sherman, D. A. Hosack, J. Yang, W. Gao, H. C. Lane, and R. A. Lempicki.** 2003. DAVID: database for annotation, visualization, and integrated discovery. Genome Biol. **4:**P3.
15. **Dreyfus, D., M. Nagasawa, E. Gelfand, and L. Ghoda.** 2005. Modulation of p53 activity by IκBα: evidence suggesting a common phylogeny between NF-κB and p53 transcription factors. BMC Immunol. **6:**12.
16. **Duncan, M. R., S. M. Stanish, and D. C. Cox.** 1978. Differential sensitivity of normal and transformed human cells to reovirus infection. J. Virol. **28:**444–449.
17. **Ehrlich, M., W. Boll, A. Van Oijen, R. Hariharan, K. Chandran, M. L. Nibert, and T. Kirchhausen.** 2004. Endocytosis by random initiation and stabilization of clathrin-coated pits. Cell **118:**591–605.
18. **Furlong, D. B., M. L. Nibert, and B. N. Fields.** 1988. Sigma 1 protein of mammalian reoviruses extends from the surfaces of viral particles. J. Virol. **62:**246–256.
19. **Gilmore, T. D.** 1999. The Rel/NF-κB signal transduction pathway: introduction. Oncogene **18:**6842–6844.
20. **Gupta, S., and S. Sen.** 2005. Role of the NF-κB signaling cascade and NF-κB-targeted genes in failing human hearts. J. Mol. Med. [Online.] doi: 10.1007/s00109-005-0691-z.
21. **Gurumurthy, S., A. Goswami, K. M. Vasudevan, and V. M. Rangnekar.** 2005. Phosphorylation of Par-4 by protein kinase A is critical for apoptosis. Mol. Cell. Biol. **25:**1146–1161.
22. **Hayden, M. S., and S. Ghosh.** 2004. Signaling to NF-κB. Genes Dev. **18:**2195–2224.
23. **Henderson, Y. C., M. Chou, and A. B. Deisseroth.** 1997. Interferon regulatory factor 1 induces the expression of the interferon-stimulated genes. Br. J. Haematol. **96:**566–575.
24. **Hiscott, J., N. Grandvaux, S. Sharma, B. R. Tenoever, M. J. Servant, and R. Lin.** 2003. Convergence of the NF-κB and interferon signaling pathways in the regulation of antiviral defense and apoptosis. Ann. N. Y. Acad. Sci. **1010:**237–248.
25. **Hiscott, J., H. Kwon, and P. Genin.** 2001. Hostile takeovers: viral appropriation of the NF-κB pathway. J. Clin. Investig. **107:**143–151.
26. **Horvath, C. M.** 2000. STAT proteins and transcriptional responses to extracellular signals. Trends Biochem. Sci. **25:**496–502.
27. **Imazu, T., S. Shimizu, S. Tagami, M. Matsushima, Y. Nakamura, T. Miki, A. Okuyama, and Y. Tsujimoto.** 1999. Bcl-2/E1B 19 kDa-interacting protein 3-like protein (Bnip3L) interacts with Bcl-2/Bcl-xL and induces apoptosis by altering mitochondrial membrane permeability. Oncogene **18:**4523–4529.
28. **Kamasani, U., and G. C. Prendergast.** 2005. Genetic response to DNA damage: proapoptotic targets of RhoB include modules for p53 response and susceptibility to Alzheimer's disease. Cancer Biol. Ther. **4:**282–288.
29. **Laemmli, U. K.** 1970. Cleavage of structural proteins during the assembly of the head of bacteriophage T4. Nature **227:**680–685.
30. **Li, Z., J. Niu, T. Uwagawa, B. Peng, and P. J. Chiao.** 2005. Function of polo-like kinase 3 in NF-κB-mediated proapoptotic response. J. Biol. Chem. **280:**16843–16850.
31. **Lipshutz, R. J., S. P. Fodor, T. R. Gingeras, and D. J. Lockhart.** 1999. High density synthetic oligonucleotide arrays. Nat. Genet. **21:**20–24.
32. **Liu, A.-X., G. J. Cerniglia, E. J. Bernhard, and G. C. Prendergast.** 2001. RhoB is required to mediate apoptosis in neoplastically transformed cells after DNA damage. Proc. Natl. Acad. Sci. USA **98:**6192–6197.
33. **Liu, A. X., N. Rane, J. P. Liu, and G. C. Prendergast.** 2001. RhoB is dispensable for mouse development, but it modifies susceptibility to tumor formation as well as cell adhesion and growth factor signaling in transformed cells. Mol. Cell. Biol. **21:**6906–6912.
34. **Liu, G., A. E. Loraine, R. Shigeta, M. Cline, J. Cheng, V. Valmeekam, S. Sun, D. Kulp, and M. A. Siani-Rose.** 2003. NetAffx: Affymetrix probe sets and annotations. Nucleic Acids Res. **31:**82–86.
35. **Lopez, C. D., Y. Ao, L. H. Rohde, T. D. Perez, D. J. O'Connor, X. Lu, J. M. Ford, and L. Naumovski.** 2000. Proapoptotic p53-interacting protein 53BP2 is induced by UV irradiation but suppressed by p53. Mol. Cell. Biol. **20:**8018–8025.
36. **Ma, S., J. Charron, and R. L. Erikson.** 2003. Role of Plk2 (Snk) in mouse development and cell proliferation. Mol. Cell. Biol. **23:**6936–6943.
37. **Nibert, M. L., and L. A. Schiff.** 2001. Reoviruses and their replication, p. 1679–1728. *In* D. M. Knipe and P. M. Howley (ed.), Fields virology, 4th ed. Lippincott Williams & Wilkins, Philadelphia, Pa.
38. **Oberhaus, S. M., R. L. Smith, G. H. Clayton, T. S. Dermody, and K. L. Tyler.** 1997. Reovirus infection and tissue injury in the mouse central nervous system are associated with apoptosis. J. Virol. **71:**2100–2106.
39. **O'Donnell, S. M., M. W. Hansberger, J. L. Connolly, J. D. Chappell, M. J. Watson, J. M. Pierce, J. D. Wetzel, W. Han, E. S. Barton, J. C. Forrest, T. Valyi-Nagy, F. E. Yull, T. S. Blackwell, J. N. Rottman, B. Sherry, and T. S. Dermody.** 2005. Organ-specific roles for transcription factor NF-κB in reovirus-induced apoptosis and disease. J. Clin. Investig. **115:**2341–2350.
40. **Pahl, H. L.** 1999. Activators and target genes of Rel/NF-κB transcription factors. Oncogene **18:**6853–6866.
41. **Pine, R., A. Canova, and C. Schindler.** 1994. Tyrosine phosphorylated p91 binds to a single element in the ISGF2/IRF-1 promoter to mediate induction by IFN alpha and IFN gamma, and is likely to autoregulate the p91 gene. EMBO J. **13:**158–167.
42. **Rodgers, S. E., J. L. Connolly, J. D. Chappell, and T. S. Dermody.** 1998. Reovirus growth in cell culture does not require the full complement of viral proteins: identification of a σ1s-null mutant. J. Virol. **72:**8597–8604.
43. **Samuels-Lev, Y., D. J. O'Connor, D. Bergamaschi, G. Trigiante, J.-K. Hsieh, S. Zhong, I. Campargue, L. Naumovski, T. Crook, and X. Lu.** 2001. ASPP proteins specifically stimulate the apoptotic function of p53. Mol. Cell **8:**781–794.
44. **Sen, G. C.** 2001. Viruses and interferons. Annu. Rev. Microbiol. **55:**255–281.
45. **Silverman, N., and T. Maniatis.** 2001. NF-κB signaling pathways in mammalian and insect innate immunity. Genes Dev. **15:**2321–2342.
46. **Sironi, J. J., and T. Ouchi.** 2004. STAT1-induced apoptosis is mediated by caspases 2, 3, and 7. J. Biol. Chem. **279:**4066–4074.
47. **Smith, M. L., J. M. Ford, M. C. Hollander, R. A. Bortnick, S. A. Amundson, Y. R. Seo, C.-X. Deng, P. C. Hanawalt, and A. J. Fornace, Jr.** 2000. p53-mediated DNA repair responses to UV radiation: studies of mouse cells lacking p53, p21, and/or gadd45 genes. Mol. Cell. Biol. **20:**3705–3714.
48. **Stark, G. R., I. M. Kerr, B. R. Williams, R. H. Silverman, and R. D. Schreiber.** 1998. How cells respond to interferons. Annu. Rev. Biochem. **67:**227–264.
49. **Strong, J. E., and P. W. Lee.** 1996. The v-erbB oncogene confers enhanced cellular susceptibility to reovirus infection. J. Virol. **70:**612–616.
50. **Sturzenbecker, L. J., M. L. Nibert, D. B. Furlong, and B. N. Fields.** 1987. Intracellular digestion of reovirus particles requires a low pH and is an essential step in the viral infectious cycle. J. Virol. **61:**2351–2361.
51. **Tamura, T., M. Ishihara, M. S. Lamphier, N. Tanaka, I. Oishi, S. Aizawa, T. Matsuyama, T. W. Mak, S. Taki, and T. Taniguchi.** 1995. An IRF-1-dependent pathway of DNA damage-induced apoptosis in mitogen-activated T lymphocytes. Nature **376:**596–599.
52. **Tan, K. O., K. M. L. Tan, S.-L. Chan, K. S. Y. Yee, M. Bevort, K. C. Ang, and V. C. Yu.** 2001. MAP-1, a novel proapoptotic protein containing a BH3-like motif that associates with Bax through its Bcl-2 homology domains. J. Biol. Chem. **276:**2802–2807.
53. **Tanaka, N., M. Ishihara, M. Kitagawa, H. Harada, T. Kimura, T. Matsuyama, M. S. Lamphier, S. Aizawa, T. W. Mak, and T. Taniguchi.** 1994. Cellular commitment to oncogene-induced transformation or apoptosis is dependent on the transcription factor IRF-1. Cell **77:**829–839.
54. **Tanaka, N., M. Sato, M. S. Lamphier, H. Nozawa, E. Oda, S. Noguchi, R. D. Schreiber, Y. Tsujimoto, and T. Taniguchi.** 1998. Type I interferons are essential mediators of apoptotic death in virally infected cells. Genes Cells **3:**29–37.

55. **Taterka, J., M. Sugcliffe, and D. H. Rubin.** 1994. Selective reovirus infection of murine hepatocarcinoma cells during cell division. A model of viral liver infection. J. Clin. Investig. **94:**353–360.
56. **Tian, B., D. E. Nowak, M. Jamaluddin, S. Wang, and A. R. Brasier.** 2005. Identification of direct genomic targets downstream of the nuclear factor-κB transcription factor mediating tumor necrosis factor signaling. J. Biol. Chem. **280:**17435–17448.
57. **Tian, B., Y. Zhang, B. A. Luxon, R. P. Garofalo, A. Casola, M. Sinha, and A. R. Brasier.** 2002. Identification of NF-κB-dependent gene networks in respiratory syncytial virus-infected cells. J. Virol. **76:**6800–6814.
58. **Tong, T., J. Ji, S. Jin, X. Li, W. Fan, Y. Song, M. Wang, Z. Liu, M. Wu, and Q. Zhan.** 2005. Gadd45a expression induces Bim dissociation from the cytoskeleton and translocation to mitochondria. Mol. Cell. Biol. **25:**4488–4500.
59. **Tyler, K. L.** 2001. Mammalian reoviruses, p. 1729–1745. *In* D. M. Knipe and P. M. Howley (ed.), Fields virology, 4th ed. Lippincott Williams & Wilkins, Philadelphia, Pa.
60. **Tyler, K. L., M. K. Squier, S. E. Rodgers, S. E. Schneider, S. M. Oberhaus, T. A. Grdina, J. J. Cohen, and T. S. Dermody.** 1995. Differences in the capacity of reovirus strains to induce apoptosis are determined by the viral attachment protein σ1. J. Virol. **69:**6972–6979.
61. **Virgin, H. W., IV, R. Bassel-Duby, B. N. Fields, and K. L. Tyler.** 1988. Antibody protects against lethal infection with the neurally spreading reovirus type 3 (Dearing). J. Virol. **62:**4594–4604.
62. **Virgin, H. W., K. L. Tyler, and T. S. Dermody.** 1997. Reovirus, p. 669–699. *In* N. Nathanson (ed.), Viral pathogenesis. Lippincott-Raven, New York, N.Y.
63. **Webster, G. A., and N. D. Perkins.** 1999. Transcriptional cross talk between NF-κB and p53. Mol. Cell. Biol. **19:**3485–3495.
64. **Zhang, Y., B. A. Luxon, A. Casola, R. P. Garofalo, M. Jamaluddin, and A. R. Brasier.** 2001. Expression of respiratory syncytial virus-induced chemokine gene networks in lower airway epithelial cells revealed by cDNA microarrays. J. Virol. **75:**9044–9058.